International Research Journal of Engineering and Technology (IRJET) e-ISSN: 2395-0056
Volume: 12 Issue: 09 | Sep 2025 www.irjet.net p-ISSN: 2395-0072

A BEVEL GEAR ROOT BENDING STRESS MODEL

[1]Edward E. Osakue & [1]Rasoul Saneifard

[1]Department of Engineering, Texas Southern University, Houston, Texas, USA

Abstract

A reversed Lewis root bending stress capacity model for bevel gears is presented. The model is developed from first principle based on the Tredgold's approximation of a bevel gear. The approximation conceptually transforms a bevel gear into a spur gear. The load distribution of the bevel gear facewidth is assumed to be triangular so that the stress at the gear is constant over the facewidth. Six design cases of root bending stress computations from different references are done using the new and AGMA models. The stress estimates from the new and AGMA models were compared. The stress deviations associated with the pinions in the gearsets for the design problem examples vary between -14 to -4%, approximately. Based on the values of the deviations for the pinion stresses, the new root bending stress model verification may be said to be favorable when compared with AGMA stress values. However, the root bending stress predictions are relatively less conservative in values.

Keywords: *Bending, fatigue failure, nominal helix angle, base helix angle, virtual plane, Lewis stress factor*

1.0 Introduction

A bevel gear has teeth cut on a conical pitch surface, making the tooth to vary in thickness and height from the front end or toe to the back end or heel. A bevel gearset consists of a pinion (smaller gear) and a ring gear (larger gear). The common types of bevel gears are straight and helical gears. The teeth of straight bevel gears are straight on the conical disk surface. Helical bevel gears have curved teeth on conical disk surfaces and include skew, spiral, zerol, and hypoid bevel gears [1, 2]. Skew bevel gears have a constant nominal helix angle like helical cylindrical gears, while spiral and zerol gears have variable helix angle. The nominal helix angle of spiral bevel is taken as the mean spiral angle defined at the mid-facewidth of the gear. The most popular helix angle for spiral bevel gears is 35^o [3], but nominal helix angles of 20^o to 45^o may be used with the same tooth proportions as for 35^o. Though spiral bevel gears resemble helical gears, they however, do not have a true helical spiral [4, 5]. Zerol bevel gears have nominal helix angle of zero degree. Hypoid gears are spiral bevel gears with non-intersecting axes. The offset allows for more compact design and efficient power transmission at greater angles than straight bevel gears. The pressure angles in use for bevel gears can vary from 14.5^o to 25^o. Pressure angles of 20^o and higher are often used to avoid interference [1]. However, 22.5^o and 25^o pressure angles are used mainly in heavy-duty drives [6]. In North America, the most popular pressure angle is 20^o. The International Standardization Organization (ISO) has adopted 20^o pressure angle as the standard pressure angle, which makes it more attractive for international collaboration and commerce.

A gear tooth in a mesh during operation acts like a loaded cantilever beam as it resists the forces transmitted. In 1892, Wilfred Lewis developed a gear root bending stress model [7]. He modeled a gear tooth as a short cantilever beam on a rigid base with the transmitted load applied near the tip of the gear tooth. The maximum tensile stress occurs at the root radius on the loaded side of the gear tooth. At the gear root, the involute profile merges with a root fillet [8] which creates some stress concentration. Due to the repeated loading of a gear tooth, this region becomes the preferential site for initiation of fatigue crack. The model of Lewis is the basis of national and international gear beam strength standards. These include American Gear Manufacturers Association (AGMA), International Standardization Organization (ISO), Deutsches Institut Normung (DIN), and Japanese Industrial Standard (JIS), which have introduced modification factors into the original Lewis model.

Bending fatigue failure is one of the two most prominent modes of gear failure. Factors that can influence gear failures include transmission error, design error, manufacturing error and assembly error. Generally, severe surface wear-out in gears, which can accelerates bending fatigue failure, may be caused by thin lubrication film between two mating surfaces and the presence of debris in the lubricant. Bending fatigue failure of straight bevel pinions is the main failure mode in engineering machinery [9]. A review of bevel gear failures by Joshi and Kothari [10] concluded that bevel gears commonly fail by tooth breakage or fatigue. Such failures are largely caused by overloading, shaft misalignment, material and metallurgical deficiencies. Mohan Raj and Jayaraj [11] performed studies using distributed and concentrated loads applied at the pitch point on a bevel gear. They found that the stresses at the toe of the tooth were higher than those at the heel. Irsel [12] showed

that estimates of bevel gear root bending stresses from ISO, AGMA, DIN, and Finite Element Method (FEM) models can be significantly different in values for the same loading. Generally, ISO, DIN, and FEM root bending stress values in the study tended to be higher than AGMA values. Implementation of ISO, DIN, and AGMA in KISSsoft commercial software yielded the same trend in root bending stress values. Irsel [12] noted that FEM studies usually apply static load, not dynamic load to gear teeth. Mieth, Ulrich1, and Schlecht1 [13] formulated a solution for bevel gear contact and root bending stresses using FEM influence. The method enables the calculation of full stress tensors at any desired location in the gear and takes account of the influence of local stiffness variations. AGMA bevel gear root bending stress model estimates are considered conservative [3, 5]. Therefore the other model estimates mentioned above appear to be even more conservative than AGMA.

Estimating root bending stress in bevel gears has been a challenge as the study of Irsel indicates. Like bending stress estimates, permissible bending fatigue stress estimates from the different standards can be significantly different too. This situation may be attributed to the geometric complexities of bevel gears which make their design calculations more complicated compared to cylindrical gears [14]. The conical shape of the gear [14] and the fact that the spiral angle in helical bevel gears is not a true helix appear to greatly complicate the stress estimate. The lack of good correlation between the root bending stress estimates from the different standards seems to suggest a strong need for new root bending stress models for bevel gears. This study presents a new mathematical formulation for the beam strength capacity of bevel gears using first principles. The developed bending stress model appears to be reasonably accurate, but slightly less conservative when compared with AGMA model. It will minimize design efforts and analysis when defining initial bevel gear sizes, often needed for more detail study using FEM. The model can therefore, help to shorten design and development times, as well as reduce bevel gear design project costs.

2.0 Bevel Gear Pitch Angles

Bevel gears have teeth cut on the frustum of a cone and for two cones to roll without sliding; they must have a common apex. This ensures that the pitch surfaces of two meshing bevel gears are proportional to the distance from the common apex and allow pure rolling of the meshing bevel gears. Therefore, proper bevel gear meshing must be considered in pairs because the cone pitch angles of the gears are restricted by the gear ratio and shaft angle [15]. The angle between the center lines of the shafts carrying the bevel gears is called the shaft angle. Generally, shaft angles between 30° and 150°[2] are usually permissible subject to some gear ratio limitations. A shaft angle of 90° is the most popular in use but other angles are sometimes used.. In conventional configuration of bevel gearsets, the shaft angle is:

$$\varphi_0 = \varphi_1 + \varphi_2 \tag{1}$$

The pitch angle of a bevel gear is the angle between the face of the pitch surface and the shaft axis. When $\varphi_o \le 90^0$, the cone pitch angles are obtained as in Eq. (2) [2].

$$\tan\varphi_1 = \frac{\sin\varphi_o}{\mu + \cos\varphi_o} \qquad \tan\varphi_2 = \frac{\mu\sin\varphi_o}{1 + \mu\cos\varphi_o} \tag{2}$$

Please, observe that there are two expressions in Eq. (2), which should be referred to as Eq. (2a) and Eq. (2b) from left to right. All other equations with multiple expressions should be interpreted similarly. The definition of parameters in equations are in the Nomenclature.

When $90^0 < \varphi_o < 180^0$, then [23]:

$$\tan\varphi_1 = \frac{\sin(180^0 - \varphi_o)}{\mu - \cos(180^0 - \varphi_o)} \tag{3a}$$

$$\tan\varphi_2 = \frac{\mu\sin(180^0 - \varphi_o)}{1 - \mu\cos(180^0 - \varphi_o)} \tag{3b}$$

Note that equations (1) to (3) do not apply to bevel crown gears where $\varphi_2 = 90^0$.

Bevel gears are generally analyzed based on equivalent spur gears defined by the Tredgold's approximation. The Octoid tooth profile is often used for implementing the Tredgold's approximation [14]. Due to the spherical nature of bevel gears, a crown gear (circular rack of straight flanks) is used to generate bevel gear tooth profile. The shape generated by the circular rack is called "octoid" and is very similar to an involute, but not exactly. The octoid provides a constant ratio and makes the gears insensitive to displacements perpendicular to the pitch line. The octoid technique allows easy manufacture [14] of bevel gears by generative method. Some gear generators require pinion pitch angle above 5° [16].

3.0 Equivalent Spur Gear For Bevel Gear

The concept of equivalent spur gear for other gear types is commonly used due to the relative simplicity of a spur gear geometry compared to the other gear types. Bevel gear teeth are cut on conical surfaces and have a spherical geometry. Hence, the involute tooth profile should be developed on a spherical surface to ensure conjugate action. Developing gear teeth on a spherical surface is a very difficult task. In a

plane normal to the pitch cone angle or contact line, meshing physical bevel gears appear to be similar to those of spur gears [15]. Therefore, the "Tredgold's approximation" is almost universally accepted. It uses the cone tangent to the sphere at the pitch point on the backend of the physical bevel gear to define the pitch radius of an equivalent spur gear. The back-cone radius of the bevel gear then becomes the radius of an imaginary spur gear with teeth and pressure angle corresponding to the bevel gear. The Tredgold's approximation is accurate enough for practical purposes as long as the bevel gear has 8 or more teeth, [14, 17, 18, 19]. It is standard practice in bevel gear technology to define the size and shape of the tooth profile at the back end [14] perhaps based on Tredgold's approximation. The manufacturing dimensions of a bevel gear are based on the backend module, which is largely standardized. Fig. 1a shows the axial plane of a straight bevel gear while Fig. 1b shows the transverse plane at the back end. The basic physical gear size parameters are shown in these figures, except the module.

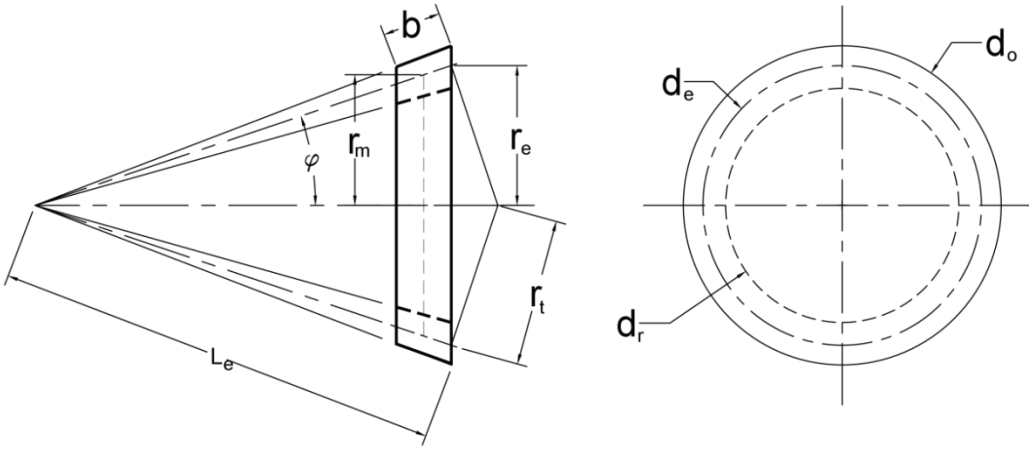

a) Axial plane b) Transverse plane

Fig. 1: Physical bevel Gear

The geometric relationships between backend dimensions of a straight bevel gear and the Tredgold's virtual spur gear are given below.

$$\frac{r_m}{r_e}=\frac{m}{m_e}=\frac{L}{L_e} \qquad d_m=d_e\left(\frac{L}{L_e}\right) \tag{4}$$

$$d_m=\frac{d_e}{K_b} \qquad K_b=\frac{L_e}{L}=\frac{L_e}{L_e-0.5b} \tag{5}$$

The parameter K_b is based on bevel geometry and differentiates bevel gears from cylindrical gears.

$$r_t=\frac{r_e}{\cos\varphi} \qquad d_t=\frac{2r_e}{\cos\varphi}=\frac{d_e}{\cos\varphi} \tag{6}$$

$$d_t=z_t m_e \qquad z_t=\frac{z}{\cos\varphi} \tag{7}$$

The gear ratio and speed ratio for bevel gears are related as expressed in Eq. (8)

$$\mu=\frac{d_{e2}}{d_{e1}}=\frac{z_2}{z_1}=\frac{N_1}{N_2} \tag{8}$$

The virtual gear ratio for straight bevel gears is given by Eq. (9)

$$\mu_t = \frac{d_{t2}}{d_{t1}} = \frac{z_2 \cos\varphi_1}{z_1 \cos\varphi_2} = \mu \frac{\cos\varphi_1}{\cos\varphi_2} \qquad (8)$$

Figs. 2a and 2b show the Tredgold's-spur gear is a spur gear that is geometrically equivalent to a straight bevel gear. The tooth profile of a regular spur gear lies in the transverse plane and is coincident with the normal plane. Similarly, the tooth profile of the Tredgold's virtual spur gear lies in the transverse plane and is coincident with the normal plane.

The basic dimensions of the Tredgold's virtual spur gear for a straight bevel gear is summarized by Eq. (9). Eq.(9b) is given for completeness. The proof is shown later in section 5.1.

$$d_t = z_t m_e \qquad b_t = \frac{b}{K_b} \qquad (9)$$

3.1 Helical Bevel Gears

The development of an equivalent spur gear for a helical bevel gear is based on two assumptions: Tredgold's approximation and helical cylindrical gear analogy. This approach results in a bi-equivalent spur gear for a helical bevel gear. The Tredgold's approximation gives the first equivalent spur gear for a straight bevel gear. A helical bevel gear is obtained a Tredgold's-spur gear as a second approximation. In this approach, the nominal helix angle of a bevel gear is defined as the mean spiral angle which is measured at the mid-facewidth of the gear tooth. A straight bevel gear can be considered as a helical bevel gear with a nominal helix angle of zero. The basic parameters for the helical bevel gears are the normal module, nominal helix angle, pitch diameter, and nominal facewidth.

$$m_e = \frac{m_n}{\cos\psi} \qquad d_e = z m_e \qquad (10)$$

The two parameters which relate a helical gear to its equivalent spur gear are the transverse pressure angle and the base helix angle [20]. When the normal pressure angle is standardized, then:

$$\phi_t = \tan^{-1}\left[\frac{\tan\phi_n}{\cos\psi}\right] \qquad \psi_b = \tan^{-1}\left[\tan\psi \cos\phi_t\right] \qquad (11)$$

According to Maitra [17], the base helix angle gives a more accurate estimate of the instantaneous radius of curvature of the equivalent spur gear for a helical gear. Therefore, the plane defined by the base helix angle will be called the virtual plane on which the pitch diameter of the virtual spur gear for a helical gear lies

$$d_v = \frac{d_t}{\cos^2\psi_b} \qquad z_v = \frac{z_t}{\cos^3\psi_b} = \frac{z}{\cos\varphi\cos^3\psi_b} \qquad (12)$$

The virtual or equivalent gear ratio of a helical bevel gearset based on Eq. (6) is:

$$\mu_v = \frac{d_{v2}}{d_{v1}} = \mu \frac{\cos\varphi_1}{\cos\varphi_2} = \mu_t \qquad (13)$$

The basic dimensions of the bi-equivalent virtual spur gear for a helical bevel gear is summarized by Eq. (14).

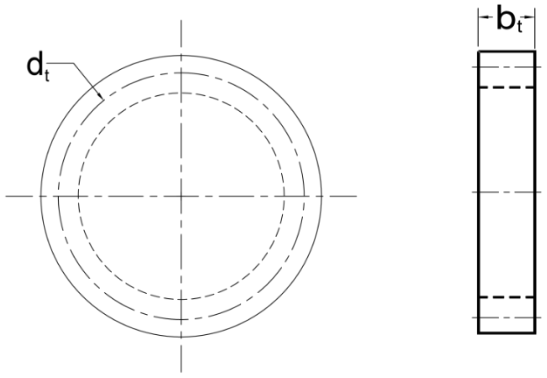

a) Transverse plane b) Axial plane

Fig. 2: Equivalent Tredgold's spur gear of a bevel gear

$$d_v = z_v m_n \qquad b_v = \frac{b}{K_b \cos\psi_b} \qquad (14)$$

3.2 Virtual Contact Ratio

The average number of gear teeth pairs in simultaneous engagement during operation is called contact ratio. The contact ratio of a bevel gearset is evaluated on the virtual plane defined by the base helix angle. The contact ratio factor for the pinion is expressed in Eq. (15a).

$$\delta_1 = 0.5\left\{\sqrt{(z_{v1}+2)^2 - z_{v1}\cos\phi_n} - z_{v1}\sin\phi_n\right\} \qquad (15b)$$

The contact ratio factor for the ring gear is expressed in Eq. (15b).

$$\delta_2 = 0.5\left\{\sqrt{(z_{v2}+2)^2 - z_{v2}\cos\phi_n} - z_{v2}\sin\phi_n\right\} \qquad (15b)$$

The expression for the contact ratio on the virtual plane for standard profile gearsets is given by Eq. (16).

$$\varpi_v = \frac{\delta_1 + \delta_2}{\pi\cos\phi_n} \qquad (16)$$

Eq. (16) yields ϖ_t, the value for straight bevel gears when z_v is equal to z_t.

4.0 Bevel Gear Forces

In the design analysis of bevel gears, the load is commonly assumed to be applied at the mid-face width. The resultant force acts somewhere between the midpoint and the back end of the tooth width [1, 5, 9, 17]. This means the force components used in design analysis are slightly conservative. It is to be noted that the complexities of the tooth profile of bevel gears make precise analysis rather very complicated and such a conservative approach is justified. Fig. 3 depicts three components of the contact force shown at the mid-plane pitch point on a straight bevel gear. These forces are the tangential, F_t;radial, F_r; and axial, F_a components of the contact force. F_a is parallel to the shaft axis, while F_t and F_r are mutually perpendicular to each other and F_a. The normal force, F_n is shown in Fig. 3 and Fig. 4. It acts normal to the gear tooth in space. The tangential force is the driving force, the radial and axial forces are generated due to the gear pressure angle and the cone pitch angle for the bevel gears. The transmitted power, torque, and tangential force are related as expressed in Eq. (17) to Eq. (18).

$$T_1 = \frac{30P_1 \times 10^3}{\pi N_1} \qquad T_2 = \mu T_1 \tag{17}$$

$$F_t = \frac{2K_b T_1 \times 10^3}{d_{e1}} = \frac{2K_b T_2 \times 10^3}{d_{e2}} \tag{18}$$

The parameter K_b in Eq. (18), transfers the point of load application from the mid-width plane to the backend plane of the actual bevel gear where the Tredgold's spur gear is defined

The radial and axial force components for a straight bevel gears are obtained from Eq. (19).

$$F_r = F_t \tan\phi_t \cos\varphi \qquad F_a = F_t \tan\phi_t \sin\varphi \tag{19}$$

These force components are modified by the nominal helix angle in helical bevel gears

Helical bevel gears are analogous to cylindrical helical gears and the forces on a bevel helical gear pair on the normal and transverse plane are shown in Fig. 4. F_o acts normal to the gear tooth and F_u acts parallel to the pitch angle.

$$F_o = \frac{F_t}{\cos\psi} \qquad F_u = F_o \sin\psi = F_t \tan\psi \tag{20}$$

The normal contact force is given by Eq. (21).

$$F_n = \frac{F_o}{\cos\phi_n} = \frac{F_t}{\cos\psi_n \cos\phi_n} \tag{21}$$

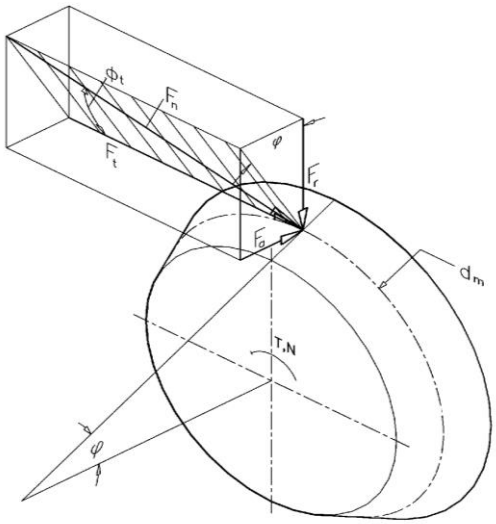

Fig. 3: Straight bevel gear forces

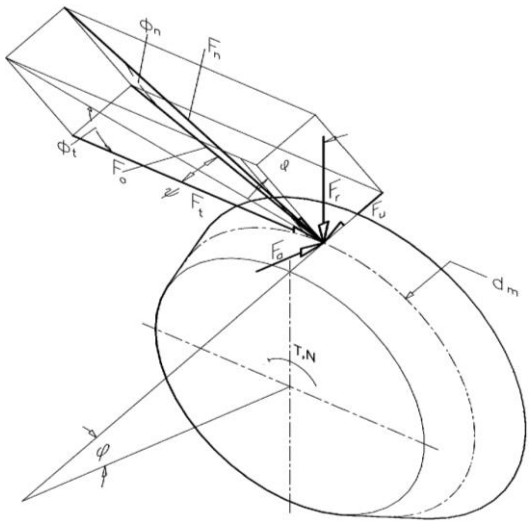

Fig. 4: Helical bevel gear forces

The radial and axial force components of a spiral bevel gear are given in Eq. (22a) and Eq. (22b) [6] when the shaft angle is 90^0.

$$F_r = F_t\left(\tan\phi_t \cos\varphi \mp \tan\psi \sin\varphi\right) \quad (22a)$$

$$F_a = F_t\left(\tan\phi_t \sin\varphi \pm \tan\psi \cos\varphi\right) \quad (22b)$$

Straight bevel gears are symmetrical in the lengthwise direction which makes for equal stresses on the faces of the gear. However, spiral bevel gears are not symmetrical in the lengthwise direction so that stresses induced in the concave and convex sides of a tooth can be different [3, 6]. Two cases can be associated with the operative forces in spiral bevel gears and they are Case I and Case II [6]. The direction of rotation of the pinion is observed from the apex point of the pitch cones of the gearset.

Case I: Left-handed pinion spiral rotates counterclockwise or right-handed pinion spiral rotates clockwise. In this case, the negative sign applies in Eq. (22a)for the radial force and positive sign applies in Eq. (22b) for axial force. The signs are reversed in each case for the gear.

Case II: Left-handed pinion spiral rotates clockwise or right-handed pinion spiral rotates counterclockwise. In this case, the positive sign applies in Eq. (22a) for the radial force and negative sign applies in Eq. (22b) for axial force. The signs are reversed in each case for the pinion.

4.1 Axial and radial Force Factors

Based on Eq. (22) axial and radial force components may be defined for bevel gears. When a pinion convex face mates with the gear concave face in Case I, the radial force factor for the pinion face is:

$$\chi_r = \frac{F_a}{F_t} = \tan\phi_t \cos\varphi + \tan\psi \sin\varphi \quad (23a)$$

And the axial force component factor is:

$$\chi_a = \frac{F_a}{F_t} = \tan\phi_t \sin\varphi - \tan\psi \cos\varphi \quad (23b)$$

The force component factors for the gear are obtained from Eq. (23a) by changing the (+) to (-) as in Eq. (23c) and Eq. (23b) by changing the (-) to (+) as in Eq. (23d).

When a pinion concave face mates with a gear convex face, in Case II, the radial force factor for the pinion face is:

$$\chi_r = \frac{F_a}{F_t} = \tan\phi_t \cos\varphi - \tan\psi \sin\varphi \quad (23c)$$

And the axial force component factor is:

$$\chi_a = \frac{F_a}{F_t} = \tan\phi_t \sin\varphi + \tan\psi \cos\varphi \quad (23d)$$

The force component factors for the gear are obtained from Eq. (23c) by changing the (-) to (+) as in Eq. (23a) and Eq. (23d) by changing the (+) to (-) as in Eq. (23b). The factors for straight bevel gears are obtained in Eq. (23) when the nominal helix angle is zero.

For spiral bevel gearsets loaded in two directions, stresses on both concave and convex faces are necessary [21]. A positive χ_a value for both pinion and gear indicates that the axial force is directed away from the cone apex and thus will prevent jamming of the gear pair during operation. This is the preferred configuration of bevel gearset in an assembly.

5.0 Root Bending Fatigue Stress Capacity Model

The objective in design verification is to assess the adequacy of a design. After initial dimensions are estimated, performance capacities of a component or assembly can be evaluated and judged for acceptability based on a minimum design factor or reliability target. If the evaluated design factor or reliability level for a failure mode is smaller or lower than the minimum value, the design is deemed inadequate otherwise it is accepted. A common performance capacity for gears is bending fatigue resistance which is one of the two prominent modes of gear failure [8, 14, 22]. Bending fatigue resistance is the capacity of a gear tooth to withstand bending load imposed by the transmitted force and its associated derivatives. Both the tangential and axial loads induce bending moment, therefore bending stresses, on a straight bevel gear tooth in addition to the direct shear stresses they cause.

Fig. 5a shows an element of a tooth assumed to be transmitting torque about the gear axis OC. We will for now consider the bending stress from only tangential force, that from the axial load with be treated latter. The radial distance to point B and gear tooth profile in the transverse plane is a linear function of the distance from the gear apex at point O.

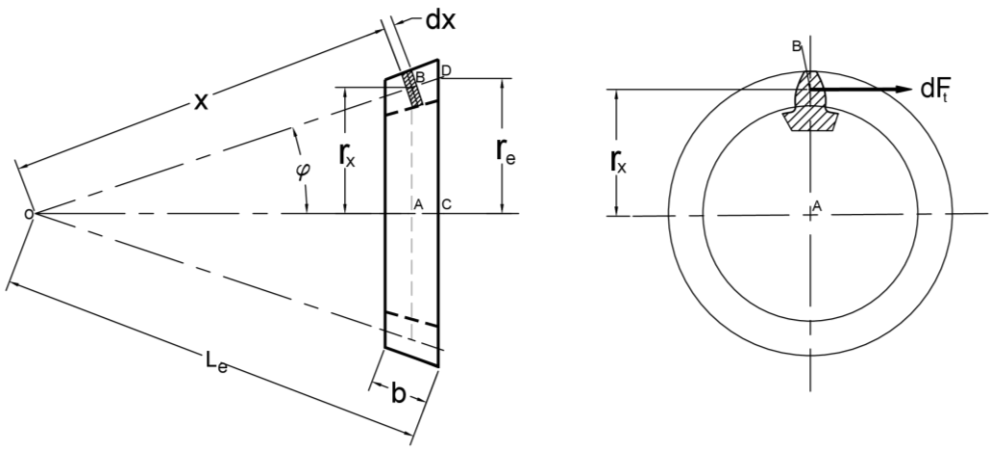

a) Axial plane b) Transverse plane

Fig. 5: Straight bevel gear bending model

From similar triangles OAB and OCD of Fig. 5a:

$$\tan\varphi = \frac{\sin\varphi}{\cos\varphi} = \frac{r_x}{\mathrm{x}\cos\varphi} = \frac{r_e}{L_e\cos\varphi} \qquad (24a)$$

That is:

$$\sin\varphi = \frac{r_x}{\mathrm{x}} = \frac{r_e}{L_e} \qquad (24b)$$

By the definition of gear module:

$$r_e = m_e z \qquad r_x = m_x z \qquad (25)$$

Substitute Eq. (24b) into Eq. (25) to obtain:

$$r_x = \left(\frac{r_e}{L_e}\right)\mathrm{x} \qquad m_x = \left(\frac{m_e}{L_e}\right)\mathrm{x} \qquad (26)$$

The bending stress analysis of straight bevel gears can be simplified by assuming that the stress is the same at any section at the root of the gear. This may be justified when the load distribution along the tooth width is assumed triangular with an apex coincident with the pitch cone apex of the bevel gear [23]. Considering only the tangential force for now, and referring to Fig. 5b and Eq. (26), the resisting elemental force against the transmitted load is:

$$dF_t = Y\sigma_{bt} m_x \mathrm{dx} \qquad dF_t = \left(\frac{Ym_e\sigma_{bt}}{L_e}\right)\mathrm{x\,dx} \qquad (27)$$

In Fig. 5b, the resisting elemental torque against the transmitted load is:

$$dT \times 10^3 = r_x dF_t = \left(\frac{Ym_e r_e \sigma_{bt}}{L_e^2}\right)\mathrm{x}^2\mathrm{dx} \qquad (28a)$$

The multiplier 10^3 is used to convert the transmitted torque from Nm to Nmm for consistency of dimensional units of the design parameters in Eq. (27). The transmitted toque is obtained by integrating Eq.(27) as indicated below.

$$T \times 10^3 = \frac{Ym_e r_e \sigma_{bt}}{L_e^2}\int_{L_e-b}^{L_e}\mathrm{x}^2\mathrm{dx} = \frac{Ym_e r_e \sigma_{bt}}{L_e^2}\left[\frac{\mathrm{x}^3}{3}\right]_{L_e-b}^{L_e} \qquad (28b)$$

When the limits of integration are applied and simplification done Eq. (29) is obtained.

$$T \times 10^3 = Ym_e r_e \sigma_{bt} b\left[1 - \frac{b}{L_e} + \frac{1}{3}\left(\frac{b}{L_e}\right)^2\right] \qquad (29)$$

Now:

$$\left[1 - \frac{0.5b}{L_e}\right]^2 = 1 - \frac{b}{L_e} + \frac{1}{4}\left(\frac{b}{L_e}\right)^2 \qquad \frac{1}{K_b} = \left[1 - \frac{0.5b}{L_e}\right] \qquad (30)$$

By comparison of the bracketed term of Eq. (29) and Eq. (30a), it may be assumed that:

$$1 - \frac{b}{L_e} + \frac{1}{3}\left(\frac{b}{L_e}\right)^2 \approx \left[1 - \frac{0.5b}{L_e}\right]^2 = \left(\frac{1}{K_b}\right)^2 \qquad (31)$$

The error in the approximation above is $\frac{1}{12}\left(\frac{b}{L_e}\right)^2$.

Generally, $\frac{b}{L_e} \le \frac{1}{3}$ in bevel gear design and the relative error in the approximation is about 1.32% and is quite negligible. From Eq. (29) and Eq. (31):

$$T \times 10^3 = Ym_e b\sigma_{bt}\frac{d_e}{2}\left(\frac{1}{K_b}\right)^2 \qquad \sigma_{bt} = \frac{2K_b^2 T \times 10^3}{m_e b d_e Y} \qquad (32)$$

5.1 Tredgold's Spur Gear Facewidth

The original Lewis and AGMA [24] root bending stress models are based on the tangential force, not the torque transmitted as shown in Eq. (32). Eq. (32b) can be transformed into a force-based version as:

$$\sigma_{bt} = \frac{K_b F_t}{m_e b Y} \qquad \sigma_{bt} = \frac{F_t}{m_e b_t Y} \qquad b_t = \frac{b}{K_b} \qquad (33)$$

A spur gear has a constant module along the gear facewidth but a bevel gear has a variable module over the facewidth. Therefore, the parameter b_t is the equivalent nominal facewidth of a straight bevel gear when treated as a spur according to Tredgold's model. Since the parameter K_b is greater than unity, b_t is always smaller than the facewidth of a spur gear of the same nominal width size. Consequently, the load capacity of a bevel of the same nominal width size as that a spur gear will be less. The parameter K_b is in this regard is a geometric scaling factor and helps to completely define the size of the equivalent spur of a straight bevel gear.

5.2 Modified Lewis Bending Stress Model for Straight Bevel Gear

Eq. (32b) gives the Lewis root bending stress of a straight bevel gear tooth induced by only the tangential force component without consideration of a stress concentration factor. In Lewis days, the concept and relevance of stress concentration was unknown. For objects under fatigue load, stress concentration cannot be ignored, especially for steel and plastic materials that are sensitive to stress concentration effects. Since the consideration for now is limited to tangential bending, Eq. (32b) can be modified with the normal or bending stress concentration factor. Also, a modified Lewis form factor called Lewis stress factor can be introduced in Eq. (32b). Consequently, Eq. (34) gives a modified Lewis root bending stress model for straight bevel gears.

$$\sigma_{bt} = \frac{2k_\sigma Y_b K_b^2 T \times 10^3}{m_e b d_e} \qquad \sigma_{bt} = \frac{k_\sigma Y_b K_b F_t}{m_e b} \qquad (34)$$

The Lewis stress factor is given by Eq. (35).

$$Y_b = \frac{1}{Y} \qquad Y_b = f(x, z_t) \qquad (35)$$

The Lewis stress factor Y_b is adopted from a JIS [15, 25] gear design standard and the values can be read from a graph given in the Appendix.

5.3 Axial Bending and Shear Stresses

The above analysis focuses only on the tangential force and the radial force which causes compression of the gear tooth through the AGMA J-factor [24] but not the axial force, explicitly. Also ignored are the shear stresses caused by both tangential and axial forces. These stresses are now considered next. Consider Fig. 6 where the gear tooth is treated as a cantilever beam with tangential and axial forces acting on it. The loads are assumed to be applied at the tip of the gear tooth located by the moment arm l_c .The axial force creates additional bending stress at the gear root as indicated in Fig. 6b. Hence the bending stress contribution from the axial load needs consideration.

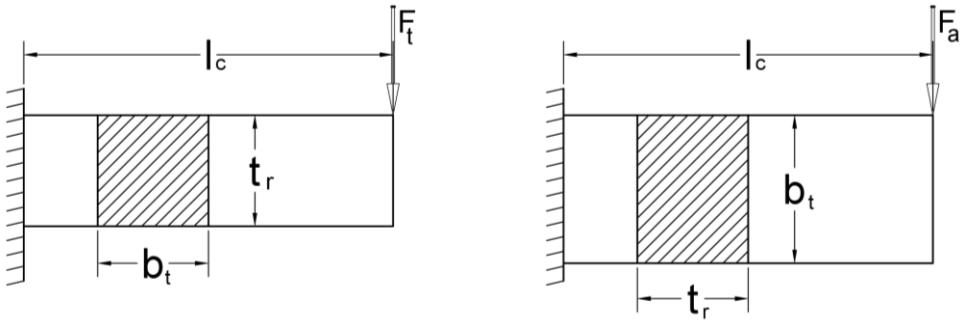

a) Transverse loading b) Axial loading

Fig. 6: Cantilever models of gear tooth in bending

From Fig. 6a, the bending stress from the tangential load component is:

$$\sigma_{bt} = \frac{F_t\, l_c}{Z_t} \qquad Z_t = \frac{b_t\, t_r^2}{6} \tag{36}$$

From Fig. 6b, the bending stress from the axial load component is:

$$\sigma_{ba} = \frac{F_a\, l_c}{Z_a} = \frac{F_t\, l_c \chi_a}{Z_a} \qquad Z_a = \frac{t_r b_t^2}{6} = \left(\frac{b_t}{t_r}\right) Z_t \tag{37}$$

Substituting Eq. (9) in Eq. (10), we have:

$$\sigma_{ba} = \frac{F_t\, l_c \chi_a}{Z_t}\left[\frac{t_r}{b_t}\right] = \sigma_{bt}\left[\frac{K_b t_r}{b}\right]\chi_a \tag{38}$$

Because of the rectangular shape of the gear tooth section at the root, the total bending stress from the tangential and axial forces is [26]:

$$\sigma_b = \sigma_{bt} + \sigma_{ba} = \sigma_{bt}\left[1 + \left(\frac{t_r K_b}{b}\right)\chi_a\right] \tag{39}$$

5.3.1 Direct Shear Stresses

The tangential and axial force components create direct shear stresses also. To account for these stresses, we will consider the equivalent spur gear of a bevel to be loaded by tangential and axial forces, though actual spur gears do not experience axial loads. Stress concentration is expected due to the geometric discontinuity caused by the root fillet; therefore, a stress concentration factor should be included in the model. It should be noted that shear stresses are assumed uniform over the section but modified by the stress concentration factor. The direct shear stress induced by the tangential load is:

$$\tau_{st} = \frac{F_t\, k_\tau}{b_t t_r} = \frac{K_b F_t\, k_\tau}{b\, t_r} \tag{40}$$

k_t is a stress combination factor that accounts for direct shear stresses from axial and tangential loads.
The direct shear stress from the axial load is:

$$\tau_{sa} = \frac{F_a\, k_\tau}{b_t t_r} = \frac{K_b F_t\, k_\tau}{b\, t_r}\chi_a \tag{41}$$

The resultant shear stress is:

$$\tau_s = \sqrt{\tau_{st}^2 + \tau_{sa}^2} = \frac{K_b F_t\, k_\tau}{b\, t_r}\sqrt{1+\chi_a^2} \tag{42}$$

Substitute for F_t in Eq. (xxx) from the bending stress equation of Eq. (xxx):

$$\tau_s = \sigma_{bt}\left(\frac{m_e k_\tau K_b}{t_r Y_b}\right)\sqrt{1+\chi_a^2} \tag{43}$$

5.3.2 Equivalent Tensile Root Stress

Equivalent tensile stress may be based on distortion energy theory for ductile materials [14, 27]. Most gears are made from ductile materials, so the equivalent tensile stress at the tooth root may be estimated by applying the distortion energy theory. For a plane stress situation, the equivalent tensile stress is given by Eq. (44a). Substituting Eq. (39) and Eq. (43) into Eq. (44a), Eq. (44b) is obtained.

$$\sigma_t = \sqrt{\sigma_b^2 + 3\tau_s^2} \qquad \sigma_t = \frac{K_b F_t\, k_\sigma k_t Y_b}{b m_e} \tag{44}$$

The parameter k_t is given by Eq. (45) .

$$k_t = \sqrt{\left[1+\left(\frac{t_r}{b}K_b\chi_a\right)\right]^2 + 3\left[\left(\frac{m_e}{t_r}\frac{k_\tau K_b}{k_\sigma Y_b}\right)^2\left(1+\chi_a^2\right)\right]} \tag{45}$$

The gear root thickness may be estimated [26] as:

$$t_r = m_e \kappa \qquad \kappa = \sqrt{\frac{6\lambda_a}{Y_b}} \tag{46}$$

A method for estimating λ_a using standard rack tooth profile is described in [28] and it has a value of 1.8321 for JIS involute spur gears of 20^0 standard pressure angle and whole depth of $2.25m$.In involute gear design, all contact between two gears occurs in the same fixed plane during meshing.

Substituting Eq. (46a) in Eq. (45), then:

$$k_t = \sqrt{\left[1+\left(\frac{\kappa m_e}{b}K_b\chi_a\right)\right]^2 + 3\left[\left(\frac{k_\tau K_b}{\kappa k_\sigma Y_b}\right)^2\left(1+\chi_a^2\right)\right]} \tag{46}$$

When load sharing is taken into account, Eq. (44b) becomes:

$$\sigma_t = \frac{k_\sigma Y_b k_t K_b F_t}{\varpi_t b_e m_e} \tag{47}$$

When the tangential force is replaced with the transmitted torque in Eq. (47), then:

$$\sigma_t = \frac{2k_\sigma Y_b k_t K_b^2 T \times 10^3}{\varpi_t m_e b_e d_e} \tag{48}$$

Eq. (48) is the revised Lewis root bending stress model for a straight bevel gear based on the Tredgold's approximation.

5.4 Root Bending Stress Extension to Helical Bevel Gear

Eq. (48) is associated with the transverse plane of the straight bevel gear. In helical bevel gears, the analysis is done on the virtual plane of the bioequivalent virtual spur gear. Using applicable normal module and virtual contact ratio, the root bending stress on the virtual plane for helical bevel is then:

$$\sigma_v = \frac{2k_\sigma k_t Y_b K_b^2 T \times 10^3}{\varpi_v m_n b_e d_e} \qquad (49)$$

In helical bevel gears, the normal bending force F_o and F_t are related by the expression of Eq. (20a). Fig. 7 shows the force components on a gear at its tip in the normal and transverse planes.

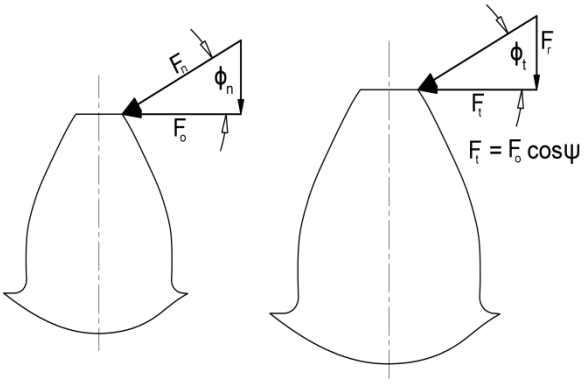

a)Normal plane b) Transverse plane
Fig. 7: Gear tooth loading in two different planes

The stress on the transverse plane in Fig. 7b is given by Eq. (50a). The normal module and transverse module are similarly related as indicate by Eq. (50b).

$$\sigma_t = \sigma_n \cos\psi \qquad m_n = m_e \cos\psi \qquad (50)$$

Assuming the stress at the gear root on the virtual plane is approximately equal to the stress at the gear root on the normal plane, then:

$$\sigma_t = \sigma_n \cos\psi \approx \sigma_v \cos\psi \qquad (51)$$

Combining Eq. (49), Eq. (50b), and Eq. (51), then:

$$\sigma_t \approx \frac{2k_\sigma Y_b k_t K_b^2 T \times 10^3}{\varpi_v m_e b_e d_e} \qquad (52)$$

5.5 Developed Facewidth of Helical Bevel Gears

Fig. 8a shows two dimensions of an arc which are the straight distance between points A and B (cord length) and the arc length between points AB. The cord length is 1.6971 mm and the arc length is 1.9902 mm and the arc length is larger than the cord length. When a gear tooth has a curvature, as it is in spiral bevel gears, the effective contact length becomes the length of an arc which is slightly larger than the gear nominal facewidth.

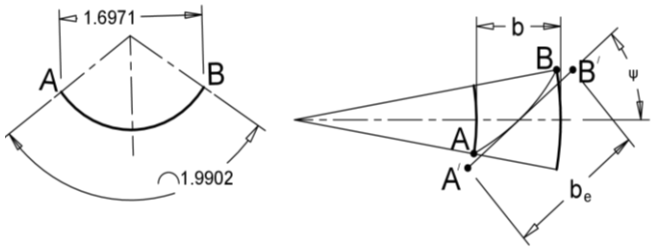

a) Arc length b) Developed length
Fig. 8: Developing the length of spiral arc

To account for the influence of the spiral curvature in spiral bevel gears, the effective facewidth of a bevel gear in contact during transmission may be expressed as in Eq. (53).

$$b_e = \lambda_\psi b \qquad b = \min(b_1, b_2) \qquad (53)$$

Physically, Eq. (53a) may be interpreted as the developed facewidth of a spiral bevel gear parallel to the line tangent to the spiral at mid-width point of the facewidth. Based on this interpretation, λ_ψ converts the contact arc into a straight line as indicated in Fig. 8b. The lengthwise curvature of spiral bevel gears gives the teeth a considerable amount of overlap, providing increased face contact ratio, tooth rigidity and adjustability to load induced deflection [30].

Fig. 8b shows the case of a spiral bevel gear facewidth and a nominal helix angle. The arc length of the spiral is the distance AB. The distance A/B/ is assumed to be the stretched out or developed length of the arc length AB. The spiral facewidth factor λ_ψ in Eq. (53a) is at least equal to unity and accounts for the developed length of the spiral arc. The spiral facewidth factor captures the effect of the lengthwise tooth curvature of spiral bevel gears on the root bending stress. AGMA [21] provides a spiral facewidth factor expression which is based on the works of Gleason, a USA specialist manufacturer of bevel gears. The AGMA [21] spiral facewidth factor expression may be approximated by Eq. (54) [3, 6, 8].

$$x = \frac{0.2788}{\log(\sin\psi)} \qquad \lambda_\psi = 0.2111\left(\frac{R_c}{L_m}\right)^x + 0.7889 \qquad (54)$$

The cutter radius in Eq. (54b) is chosen with Eq. (55a) as a guide [21, 29]. Eq. (55b) is obtained by substituting Eq. (55a) in Eq. (54b).

$$R_c \approx 1.1 L_m \sin\psi \qquad \lambda_\psi \approx 0.2111(1.1\sin\psi)^x + 0.7889 \qquad (55)$$

Table 1: Spiral Angle Factor			
Spiral Angle (deg.)	**Spiral Facewidth Factor**	**Spiral Angle (deg.)**	**Spiral Facewidth Factor**
0.10	1.186	15	1.172
0.25	1.186	20	1.168
0.50	1.185	25	1.163
1	1.184	30	1.156
2	1.183	35	1.148
3	1.182	40	1.138
5	1.180	45	1.125
10	1.176	50	1.108

Table 1 shows values of some selected nominal helix angles and spiral angle factor. Note that λ_ψ has higher values for lower nominal helix angles and slightly lower values for cutter radius greater than the assumed value in Eq. (55a). In general, the nominal helix angle tolerance is largely dependent on applications, but typically, the helix angle tolerance is ± 0.5° [31]. It is suggested that Y_ψ may be taken as 1.185 for zerol bevel gears, assuming a tolerance of ±0.5° for the nominal helix angle, ψ. Y_ψ is unity for straight and skew bevel gears [3].

5.6 Service Load Factor *(Ks)*

Experience shows that the forces acting on devices in service are generally higher than the rated or nominal values in gear drives [5, 17, 28, 32]. Practically, the design or service load is often estimated by multiplying the rated load with a service load factor which accounts for load increases during normal operations of gearsets. It does not account for peak or momentary overload. The service load factor is a load magnification factor and in gear design it may be evaluated by a multiplicative model as expressed in Eq. (56) [2, 26, 33, 34]:

$$K_s = K_a K_v K_m K_r K_p K_f \qquad (56)$$

The service load factor components K_a, K_v, K_m, and K_r are as defined in AGMA standards with similar but not identical equivalents in ISO standards. They are evaluated in this study using AGMA methods which are somewhat simpler than those of ISO. The profile shift load factor K_p [34] accounts for the influence of addendum modification or center distance adjustment on the load capacity of gears. It is a geometric parameter and is included in the service load factor because it affects both contact and bending stresses. The friction load factor K_f [26] accounts for additional load due to the presence of mesh friction. More information about the selection of K_a and the evaluation of K_v, K_m, and K_r can be found in [2, 26, 28], and AGMA documents [33].

5.7 Stress Concentration Factors

Eq. (52) incorporates a bending stress concentration factor (k_σ) and Eq. (46) incorporates both normal (k_σ) and shear stress (k_τ) concentration factors. Stress concentration gives rise to unusually high stresses near a stress raiser while much lower stress values exist on the remainder of a cross-section. Practically, some factors tend to limit stress concentration effects, and these include local plastic deformation, residual stresses, notch radius, component size, and load type [26, 28]. The effective bending or normal stress concentrator factor k_σ was estimated to be in the range of 1.25 to 1.67 [35] for cylindrical steel gears with an average of 1.46, but a value of 1.45 adopted. It is assumed that the value of k_σ for steel bevel gears is about the same as that for steel cylindrical gears. Hence a value of 1.45 for k_σ is adopted for bevel steel gears in this study. The shear stress concentration factor k_τ is in general a function of material and geometry like the normal stress concentration factor. The value of k_τ will be taken as 2 for bevel gears [35, 36].

5.8 Lewis Stress Factor

Bevel gears are different from cylindrical gears in some aspects. For instance, the shape of bevel gears generated by a circular rack is called "octoid" and is very similar to an involute, but not exactly. Hence the tooth profile of a generated bevel gear is not a true involute curve. Now, a spur gear has a constant module along the gear facewidth but a bevel gear has a variable module over the facewidth. Consequently, the backend module is larger than the frontend module, resulting in a smaller tooth thickness at the frontend. Therefore, the stress at the frontend of the tooth is likely to be higher than the value at the backend of the tooth. The smaller module at the toe gives rise to a smaller fillet radius which increases the stress concentration at the toe area. In the light of these differences with cylindrical gears, the values of the Lewis stress factor for bevel gears is expected to be different from those of cylindrical gears. The chart of Fig. A1 [15, 37] in the

Appendix A provides values of the Lewis stress factors for straight bevel gears.

5.9 Revised Lewis Root Bending Stress Capacity

Accounting for the developed facewidth and service load factor, the root bending stress estimate of Eq. (52) for bevel gears is modified into Eq. (57).

$$\sigma_t = \frac{2K_s k_\sigma Y_b k_t K_b^2 T \times 10^3}{\varpi_v m_e b d_e \lambda_\psi} \qquad (57)$$

Eq. (57) incorporates the Tredgold's approximation, Octoid approximation of involute, triangular load distribution on the bevel gear facewidth, and the integral approximation of Eq. (31). If the load distribution on the bevel gear facewidth is not triangular but constant or nearly constant, the bending stress distribution will vary over the gear facewidth. Higher stress value should be expected at the toe end since the module is smaller at that section than the other sections behind it. It should be noted that the root bending stress is evaluated separately for the pinion and ring gear.

6.0 Root Bending stress Model Applications

The bending stress capacity model of Eq. (57) was used to estimate the root bending stresses of six gear design examples taken from different references. The formulas for the bending stress estimates for the AGMA (Appendix B) and new models were coded into Microsoft Excel. The root bending stresses for the pinion and gear in a gearset were evaluated separately. The values of k_σ and k_τ used in the stress estimates are 1.45 and 2.0, respectively. The problem data for the design examples are provided in Table 2. Table 3 gives some intermediate data for evaluating the root bending stresses for the design examples. Table 4 gives the evaluated root bending stresses for the spiral bevel gears in the examples. A comparison of the root bending stress estimates from the two models is made in Table 3.

Table 2: Input Data for Numerical Examples

Parameters	Ex-1 [38]	Ex-2 [3]	Ex-3 [14]	Ex-4 [1]	Ex-5 [3]	Ex-6 [8]	Unit
Transmitted power	5.11	8.5	5.22	1.86	0.9	29.8	kW
Pinion speed	900	3000	1150	600	14000	1750	rpm
Gear speed	300	2143	350	200	6563	612.5	rpm
Normal pressure angle	20	20	20	20	20	20	deg.
Nominal helix angle	0	0	0	0	35	25	deg.
Shaft angle	90	90	90	90	90	90	deg.
Pinion teeth number	20	25	18	16	15	14	#
Gear teeth number	60	35	59	48	32	40	#
Backend module	3.175	3	2.822	3.175	1.5	4.536	mm
Pinion pitch diameter	63.5	75	50.80	50.8	22.5	63.504	mm
Gear pitch diameter	190.5	105	166.50	152.4	48	181.44	mm
Face width	31.75	21.51	26.16	25.4	8.84	25.4	mm

Table 3: Some Intermediate Parameters for Numerical Examples

Parameters	Ex-1	Ex-2	Ex-3	Ex-4	Ex-5*	Ex-6*	Unit
Pinion torque	54.22	27.06	43.36	29.60	0.61	162.61	Nm
Pitch velocity	2.99	11.78	3.06	1.60	16.49	5.82	m/s
Gear profile grade (ISO)	11	8	10	11	7	9	#
Gear ratio	3.0	1.40	3.278	3.0	2.133	2.857	#
Bevel gear factor	1.188	1.200	1.177	1.188	1.200	1.152	#
Virtual contact ratio	1.739	1.722	1.727	1.702	1.756	1.720	#
Application factor	1.000	1.000	1.000	1.500	1.500	1.000	#

Dynamic overload factor	1.328	1.284	1.266	1.242	1.173	1.211	#
Mesh overload factor	1.256	1.103	1.104	1.104	1.085	1.088	#
Rim rigidity load factor	1.000	1.000	1.000	1.000	1.000	1.000	#
Profile load factor	1.000	1.000	1.000	1.000	1.000	1.000	#
Frictional overload factor	1.117	1.084	1.113	1.130	1.047	1.060	#
Service load factor	1.862	1.535	1.556	2.322	1.999	1.396	#
* Spiral bevel gear							

Table 4: Spiral Bevel Gear Root Bending Stresses

Condition	Example	New		AGMA		Deviation (%)	
		Pinion	Gear	Pinion	Gear	Pinion	Gear
CASE I	Ex-5	35.33	24.09	36.88	37.78	-4.22	-36.25
	Ex-6	244.10	171.20	259.76	229.20	-6.03	-25.30
CASE II	Ex-5	23.90	29.94	36.88	37.78	-35.20	-20.76
	Ex-6	184.80	192.09	259.76	229.20	-28.86	-16.19
MAXIMUM STRESS	Ex-5	35.33	29.94	36.88	37.78	-4.22	-20.76
	Ex-6	244.10	192.09	259.76	229.20	-6.03	-16.19

Table 5: Root Bending Stress Comparisons

Example	Current Model (MPa)		AGMA (MPa)		Stress Deviation (%)	
	Pinion	Gear	Pinion	Gear	Pinion	Gear
Ex-1	125.72	106.62	135.31	166.12	-7.09	-35.82
Ex-2	66.92	63.74	77.51	89.15	-13.66	-28.51
Ex-3	143.36	119.76	158.52	186.49	-9.56	-35.78
Ex-4	144.42	117.94	153.39	190.70	-5.85	-38.16
Ex-5	35.33*	29.94*	36.88	37.78	-4.22	-20.76
Ex-6	244.10*	192.09*	259.76	229.20	-6.03	-16.19
* Maximum stresses in pinion and gear						

7.0 DISCUSSION

As mentioned earlier, the gear design problems were taken from different references and the root bending stress estimates were made using Eq. (57) and AGMA model (Eq. (B1)). The examples consist of four straight bevel gearsets and two spiral bevel gearsets. The two spiral bevel gears have spiral angles of 35^o and 25^o. For the verification of predictions from Eq. (57); the results are compared with those of AGMA model [21, 24]. AGMA model is chosen for comparison because of its popular acceptance in gear technology and industry. In addition, the findings by Irsel [12] indicate that the root bending stresses of AGMA model were lower than those of ISO and FEM stresses. But AGMA bevel gear stress models are said to provide conservative estimates of bending and contact stresses for straight, zero, and spiral bevel gears [3].

The design problem data for the examples considered are shown in Table 2. Examples 1 to 4 are for straight bevel gears, while examples 5 and 6 are for spiral bevel gears. These gear parameter values were used as the input data for the evaluation of the root bending stresses for the gearsets. Table 3 provides some intermediate data on the design problem examples. In the table, the virtual contact ratio is observed to be between 1.7 and 1.76 and the service load factor is between 1.35 to 2.35. Each component of the service load factor is also provided. The frictional load factor

is between about 1.05 to 1.13. Hence, the frictional load factor increased the root bending stress estimates by about 5 to 13%. AGMA model does not consider this factor but it appears to be quite relevant.

A satisfactory gearset design ensures that both pinion and gear can safely transmit the intended load. Straight bevel gears are symmetrical in the lengthwise direction, therefore equal stresses are expected on the faces of the gears. Since the pinions in the gearsets have fewer number of teeth, the Lewis stress factors are higher than those of the ring gears. Consequently from Eq. (57), they are expected to experience higher root bending stresses than the ring gears in operations. However, spiral bevel gears are not symmetrical in the lengthwise direction and the stresses induced on the concave and convex sides of a gear tooth can be different [3]. When a spiral gearset is under reversed fatigue or bi-directional loading, the stresses on both sides of the gear teeth must be evaluated to ascertain the greater one.

Table 4 gives spiral bevel gear root bending stresses for both Case I and Case II and compares the estimates from the new and AGMA models. Case I represents uni-directional loading, while Case II represents bi-directional loading.

7.1 Stress Values Comparisons

In the spiral bevel gears, the pinion stresses of the new model in Case I compare very favorably with the pinion stresses of the AGMA estimates buy very slightly lower in values. But the stresses in the gears in CASE I from the new model are significantly lower than the AGMA values. The gear stresses of the new model in Case II compare better with the gear stresses of the AGMA estimates, but still significantly lower. The pinion stresses in CASE II are also significantly lower than the AGMA values. When the maximum stresses from Case I and Case II for the new model estimates are compared with AGMA estimates on the last two rows of Table 4, it is observed the stress deviations are now lower or more favorable, but the new model estimates are still less conservative. It appears that AGMA model values are based on the maximum stresses in either the pinion or the gear. Therefore, it is thus suggested that both Case I and Case II conditions should be investigated for spiral bevel gears at the design phase. This will ensure that the gear design is safe if the direction of gears in operation are accidentally reversed. The spiral bevel gear data in Table 5 is based on this approach.

Table 5 gives the comparison of stress value predictions form the new and AGMA models. The stress deviations associated with the pinions in the gearsets for the design problem examples vary between -14 to -4%, approximately. The stress deviation for the gears are relatively larger than those for the pinions, but are not critical for uni-direction loading of both straight and spiral bevel gears. Generally, the stress values from the new model are relatively lower than those from AGMA model. Hence, the model is slightly less conservative than AGMA model, which has been described as being somewhat conservative [3]. The new model therefore, seems quite realistic.

Based on the values of the stress deviations for straight bevel gears and the stress deviations for the maximum stresses for spiral bevel gears in Table 5, the new root bending stress model verification can be said to be very favorable. However, the stress values predicted are slightly less conservative in values. Dudley [5] observed that current bevel gear design practice in the United States tend to often outperform expectations. This appears to suggests that current United States models probably over-estimate bevel gear stresses. Similar sentiments are expressed by Childs [3]. Since the new root bending stress model appears to be less conservative than the AGMA model, it may be very attractive for applications.

The virtual plane in the model presented is based on the base helix angle for helical bevel gears. This is different and distinct from that of the normal plane which is defined by the nominal helix angle. The Tredgold's spur gear is a geometrical construct which is used to define a spur equivalence for a bevel gear. The forces on a physical bevel gear are transferred to the Tredgold's spur gear for bending stress analysis by means of the bevel gear factor. Consequently, the bending stress on the Tredgold's spur is being used to predict or simulate the bending stress on the physical bevel gear. Straight bevel gears become Tredgold's spur gears by one transformation, while helical bevel gears become Tredgold's helical spur gears by a double transformation.

7.2 Some Features of Current Model

Current AGMA, JIS, and ISO models generally use different design charts for straight bevel gears and spiral bevel gears, with a different chart required for each spiral angle. Thus a large number of charts would be needed in practice for several spiral angles. This may be one of the reasons why a spiral angle of 35^{o} is most popular. The Lewis stress factor from Fig. A1 is for straight bevel gears. However, it was used in the new model for spiral bevel gears also. In the new model, the stress combination factor effectively accommodates any spiral angle for bevel gears. Therefore, a separate chart is not required for each spiral angle. Thus, the use of the stress combination factor of Eq. (46) combined with the Lewis stress factor values from Fig. A1 reduces the

number of design charts for bevel gear design analysis to just one chart for all types of bevel gears. The is a great benefit from the new bevel gear root bending stress model.

The new bevel gear root bending stress model accommodates both axial and shear stresses explicitly in the stress combination factor, something lacking in current bevel gear design standards. Incorporated in the stress combination factor of Eq. (46) is the shear stress concentration factor. This is entirely new in gear bending stress analysis and makes the new model an improvement on the current available bevel gear root bending stress models. It should be noted that the base helix angle is used in the estimation of the virtual number of gear teeth in Eq. (12b) or Eq. (A1b). Current bevel gear design standards use the nominal helix or spiral angle for the estimation of the virtual number of gear teeth. According to Maitra [17], the base helix angle gives a more accurate estimate of the virtual diameter of helical gears and hence should also give a more accurate number of the virtual number of gear teeth.

Eq. (33c) gives the equivalent facewidth of the Tredgold's spur gear. In Table 3, the bevel gear factor, K_b is in the range of 1.152 to 1.20 with an average of 1.184.The parameter is usually greater than unity, indicating that b_t will always be smaller than the facewidth of a spur gear of the same nominal size. Consequently, the load capacity of a bevel gear of the same nominal facewidth size as a spur gear will be less for the same bending stress. In order to transmit the same tangential load, the facewidth of a straight bevel gear will be approximately that of a spur gear multiplied by K_b. According to experimental data, the load-carrying capacity of bevel gear drives amounts to about 85% of that spur gear drives [23, p. 159]. The load capacity of bevel gears is often stated as being about 85% of a spur gear [15, 36, 37]. For the average K_b of 1.184 in Table 3, the reciprocal is 0.845. Therefore, for the examples studied, the load capacity of a bevel gear is predicted to be about 84.5% of that a spur gear of the same nominal size, on the average. This prediction is very close to the experimental value of 85%. This appears to be an indirect verification of the new root bending stress model.

8.0 Conclusions

A reversed Lewis root bending stress capacity model for bevel gears is presented. It incorporates the Tredgold's approximation and the Octoid approximation of involute. It also assumes a triangular load distribution on the bevel gear facewidth, and an integral approximation of Eq. (31). If the load distribution on the bevel gear facewidth is not triangular but constant or nearly constant, the bending stress distribution will vary over the gear facewidth. Higher stress value would be expected at the toe end since the module is smaller at that section than the other sections behind it. The root bending stress is evaluated separately for the pinion and ring gear.

Six design cases of bending stress computations from different references are done using the new and AGMA models. The values of k_σ and k_τ used in the stress estimates are 1.45 and 2.0, respectively. The stress estimates from the new and AGMA models were compared, noting the deviations of the new model estimates from AGMA values. The stress deviations associated with the pinions in the gearsets for the design problem examples vary between -14 to -4%, approximately. Generally, the stress values from the new models are relatively lower than those from AGMA model. The spiral bevel gear stress estimates appear to the about the same as those of AGMA models. Based on the values of the deviations for the pinion stresses, the new root bending stress model verification can be said to be in favorable comparison with AGMA stress values. However, they are less conservative in values.

According to Dudley [5, p. 3.87], stresses estimated using the general practice developed in the U.S. for bevel gears predict quick failure but such gears are known to be satisfactory in service. According to him "This is a serious problem." This seems to suggest that current U.S. rating practice of bevel gears may be quite conservative. Therefore, the new root bending stress model for bevel gears presented in this paper seems to address this serious problem by providing slightly less conservative stress estimates.

Nomenclature

Subscripts: 1 for pinion; 2 for ring gear

b – nominal facewidth (mm)

b_e – effective facewidth (mm)

b_t – Tredgold's spur gear facewidth (mm)

b_v – virtual gear facewidth (mm)

d_e – backend pitch diameter(mm)

d_m – mean pitch diameter (mm)

d_t – Tredgold'spitch diameter (mm)

d_v – virtual helical spur gear diameter (mm)

dx – elemental facewidth thickness (mm)

F_t – transmitted or tangential force (N)

F_r – radial force component (N)

F_a – axial force component (N)
F_n – normal force component (N)
F_o – bending force component in normal plane (N)
F_u – pitch angle force component (N)
dF_t – elemental tangential force component (N)
$f()$ – function of
J – AGMA modified Lewis form factor
K_b – bevel gear factor
K_a – load application factor
K_f – frictional load factor
K_m – mesh overload factor
K_p – profile shift load factor
K_r – rigidity load factor
K_v – internal overload load factor
K_s – service load factor
k_t – stress combination factor
k_σ – tensile or normal stress concentration factor
k_τ – shear stress concentration factor
l_c – bending moment arm (mm)
L – mean cone distance of gear
L_e – back end cone distance of gear
m_n – normal module (mm)
m_e – back end module (mm)
N_1 – rotational speed of pinion (rpm)
P_1 – power transmitted by pinion (kW)
r_e – backend pitch radius (mm)
r_m – mean pitch radius (mm)
r_x – elemental facewidth pitch radius (mm)
r_t – Tredgold's pitch radius (mm)
R_c – cutter radius
t_r – gear root thickness (mm)
T_1 – torque transmitted by pinion (Nm)
V_t – tangential mesh speed (m/s)
x – elemental facewidth pitch distance (mm)
x – spiral angle exponent
x_n – profile shift factor on normal plane
Y – modified Lewis form factor for spur gear
Y_b – Lewis stress factor from JIS
z – number of physical teeth on gear
z_t – Tredgold'snumber of gear teeth
z_v – number of virtual teeth of gear
χ_a – axial force component factor
χ_r – radial force component factor
λ_ψ – spiral facewidth factor
ϕ_n – normal pressure angle (deg.)
ϕ_t – transverse pressure angle (deg.)
ψ – nominal helix angle
ψ_b – base helix angle
φ_o – shaft angle
φ – pitch angle
μ – gear or speed ratio
μ_t – Tredgold's gear ratio
μ_v – virtual gear ratio
δ – virtual contact ratio factor
κ – tooth root thickness factor
τ_s – combined direct shear stress (MPa)
τ_{sa} – axial direct shear stress (MPa)
τ_{st} – tangential direct shear stress (MPa)
ϑ_m – mesh friction factor
λ_a – bending moment arm factor
α_r – effective radial load component factor
ϖ_v – virtual contact ratio
ϖ_t – Tredgold's contact ratio
σ_b – combined root bending stress (MPa)
σ_{bt} – tangential root bending stress (MPa)
σ_{ba} – axial root bending stress (MPa)
σ_n – normal plane tensile root bending stress (MPa)
σ_t – effective tensile root bending stress (MPa)
σ_v – virtual plane tensile root bending stress (MPa)

References

[1] Mott, R. L. *Machine Elements in Mechanical Design*, 4th ed. SI, Pearson Prentice Hall, New York. 2004, p. 333.

[2] Osakue, Edward E.; Anetor, Lucky; and Harris, Kendall, *Contact Stress In Helical Bevel Gears*, (2021). https://digitalscholarship.tsu.edu/facpubs/38.

[3] Childs, P. R. N., *Bevel Gears, Mechanical Design Engineering Handbook*, Butterworth Heinemann Elsevier, Boston, Chap. 10, 2014.

[4] Stadtfeld, H. J., *The Basics of Spiral Bevel Gears*, Gear Technology, pp. 31 –38, 2001.

[5] Dudley, D. W., *Handbook of Practical Gear Design*, CRC Press, 2004.

[6] Shigley, J. E and Mischke, C. R. (Chief Editors), *Standard Handbook of Machine Design*, McGraw-Hill, New York, 1996, Chap. 34.16.

[7] Bommisetty, V. S. N. K, *Finite Element Analysis of Spur Gear Set, Masters*' Thesis, Mechanical Engineering Department, Cleveland State University, 2012.

[8] Schmid, S. R., Hamrock, B. J. and Jacobson, B. O., *Fundamentals of Machine Elements*, 3rd ed., CRC Press, New York, 2014, Chap. 14.p. 396.

[9] Deng Songi, Hua Lin, Han Xing-hui, and Huang Songi, *Finite Element Analysis of Contact and Bending Fatigue of a Theoretical Assembling Straight Bevel Gear Pair*, J. Cent. South Univ., 20, 279 – 292, 2013. DOI: 10:1007/s11771-013-1486y.

[10] Joshi, H. D. & Kothari, K. D., *Mode and cause of failure of a Bevel gear-A review*, Int'l Journal of Advance Engineering and Research Development (IJAERD) Volume 1 Issue 2, March 2014, e-ISSN: pp. 2348 – 4470, 2014.

[11] Mohan Raj, N., Jayaraj, M, *Design of Contact Stress Analysis in Straight Bevel Gear*, International Journal of Computational Engineering Research, Vol-03, Issue-4, 2013.

[12] Irsel, G., *Bevel Gear Strength Calculations: Comparison of ISO, AGMA, DIN, KISSsoft and FEM Methods*, Journal of the Chinese Society of Mechanical Engineers, Vol. 42, No. 3, pp. 315 – 323, 2021.

[13] Mieth1, F., Ulrich1, C., Schlecht1, B., *Stress Calculations on Bevel Gears with FEM Influence Factors*, Forsch Ingenieurwes 86:491–501,(2022); https://doi.org/10.1007/s10010-021-00550-2

[14] Collins, J. A., Busby, H., Staab, G. H., *Mechanical Design of Machine Elements and Machines*: A Failure Prevention Perspective, 2nd Edition, John Wiley and Sons, New York, 2010.

[15] KHK, *Technical Reference*, https://khkgears.net/new/gear_knowledge/gear_technical_reference/bending-strength-of-spur-and-helical-gears.html.

[16] Crosher W. P., (2012), *Bevel gears, pressure angles and their relationship*, https://gearsolutions.com/media/uploads/uploads/assets/PDF/Articles/Dec_12/1212_ToothTips.pdf.

[17] Maitra, G. M., *Fundamentals of Toothed Gearing: Handbook of Gear Design*, 2nd Edition, McGraw Hill, New Delhi, 2013.

[18] Abdoli, H. A., *Finite Element Approach to Spur, Straight Bevel and Hypoid Gear Design*, Research Report in Mechanics, University of Oslo, 2005.

[19] Shigley J. E. and Uicker, Jr, J. J., *Theory of machines and mechanisms*, McGraw-Hill, 1995. Khurmi and Gupta, (2015).

[20] Osakue, E. E. and Anetor, L., *Helical Gear Contact Fatigue Design by Spur Gear Equivalency*, Int'l Journal of Research in Engineering and Technology, Vol. 06, Issue 02, 2017.

[21] 21- ANSI/AGMA 2005-D03, *Design Manual for Bevel Gears*, pp. 40 - 41, http://allaboutmetallurgy.com/wp/wp-content/uploads/2016/12/Design-Manual-for-Bevel-Gears.pdf, 2005. Accessed March 20, 2021).

[22] Bergseth, E. *Influence of Gear Surface Roughness, Lubricant Viscosity and Quality Level on ISO 6336 Calculation of Surface Durability*, Technical Report, Department of Machine Design, Royal Institute of Technology, Stockholm, https://www.diva-portal.org/smash/get/diva2:489751/FULLTEXT01.pdf, 2009.

[23] Petrov, M., Chernilevsky, D., Berezovsky, Y. *Machine Design*, MIR, Moscow, 1988, p. 158

[24] ANSI/AGMA 2003-B97, https://www.agma.org/standards/ansi-agma-2003-b97/.

[25] JIS B0003:89, JIS B 17755:99. www.eng-tips.com,

[26] Edward E. Osakue, Anetor, L. and Harris, K., *A Parametric Study of Frictional Load Influence in Spur Gear Bending Resistance*, FME Transactions journal, (2020) 48, 294 – 306.

[27] Osakue, E. E. and Anetor, L., *Helical Gear Bending Fatigue Design*, Int'l Journal of Research in Engineering and Technology, Vol. 06, Issue 04, 2017

[28] Edward E. Osakue and Anetor, L., *Revised Lewis Bending Stress Capacity Model for Cylindrical Gears*, The Open Mechanical Engineering Journal, 2020, Vol. 14, pp. 3 - 16.

[29] Rortbart, H. A. & Brown, T. H. (2006), *Mechanical Design Handbook*, 2nd ed., McGraw-Hill, New York.

[30] Stadtfeld, H., Tribology Aspects in Angular Transmission Systems, Part VII, Gear Technology, 2011,

[31] *Helix Angle Tolerance*; https://www.practicalmachinist.com/vb/general/crossed-helical-gears-helix-angle-tolerance-309404/

[32] Edward E. Osakue, *Simplified Spur Gear Design*, Proceedings of International Mechanical Engineering Congress and Exposition 2016 IMECE, Paper Number IMECE2016-65426, Phoenix Arizona, USA November 11-17, 2016,.

[33] AGMA, *Fundamental Rating Factors and Calculation Methods for Involute Spur and Helical Gear Teeth*, ANSI/AGMA 2004-D04.

[34] Osakue, E. E. and Anetor, L. *A Comparative Study of Contact Stress from Different Standards for Some Theoretical Straight Bevel Gear Pairs*, IJRET: International Journal of Research in Engineering and Technology, https://doi.org/10.15623/ijret.2018.0708019, 2018.

[35] Osakue, E. E, *Extending Revised Lewis Gear Root Bending Stress Model to Addendum Modified Cylindrical Gears*, International Research Journal of Engineering and Technology (IRJET), 2025, Vol. 12, Iss. 7, pp. 254 – 271.

[36] Chernilevsky, D., *A Practical Course in Machine Design*, MIR, Moscow, 1990, p. 93.

[37] SDP/SI, *Elements of Metric Gear Technology*, https://www.sdp-si.com/resources/elements-of-metric-gear-technology.

[38] Budynas, R. G. and Nissbett, J. K., Shigley's *Mechanical Engineering Design*, 9th ed., McGraw Hill Education, Delhi, 2010.

APPENDIX A: Lewis Stress Factor (Y_b)

Eq. (57) incorporates the parameter Y_b , a modified form of the famous Lewis form factor. It is adopted from a Japanese Industrial Standard (JIS) for Gear design [15, 37]. Y_b is similar to the reciprocal of the AGMA *J*-factor but is independent of stress concentration factor and load sharing. Y_b is based on a tool corner radius of 0.12*m*, gear tooth whole height of 2.118*m*, and standard pressure angle of 20°. These specifications are nearly identical to those of the Gleason standards for bevel gears. Fig.A1 shows a plot of Y_b for different values of profile shift factors in the range -0.5 to 0.5, against the virtual number of teeth on a bevel gear. It is a function of the virtual number of teeth for a gear and the profile-shift factor. This summarized by Eq. (A1).

$$Y_b = f(z_v, x) \qquad z_v = \frac{z}{\cos\varphi \cos^3\psi_b} \qquad \text{(A1)}$$

The values of Y_b for profiled shifted and standard profile gears can be obtained from Fig. A1. This chart is different from that used for spur gears and provides values of Y_b slightly higher than those for spur gears for the same profile shift coefficient and virtual number of teeth.

APPENDIX B: MODIFIED AGMA BENDING STRESS CAPACITY MODEL FOR BEVEL GEARS

Based on ANSI/AGMA 2003-B97 standard [xxx], the bending stress capacity model of bevel gears may be rendered as in Eq. (B1).

$$\sigma_t = \frac{K_o k_x F_t}{m_e b Y_\psi J} \qquad \sigma_t = \frac{2K_o k_x T \times 10^3}{m_e b d_e Y_\psi J} \qquad \text{(B1)}$$

The *J* -value for bevel gears accommodates load sharing [Childs-HB], inertia ratio with gears low contact ratio, and point of load application. Note that Eq. (B1) is evaluated The size factor k_x is applied to the bending stress as indicated in

Eq. (B1). However, it may be assumed as unity in Eq. (B1) and used to modify the fatigue strength of the gear material, instead. This is the usual practice with cylindrical gears. It was assumed as unity in using Eq. (B1) in this study.

The service load factor in AGMA model is obtained as:

$$K_o = K_a K_v K_m K_r \quad \text{(B2)}$$

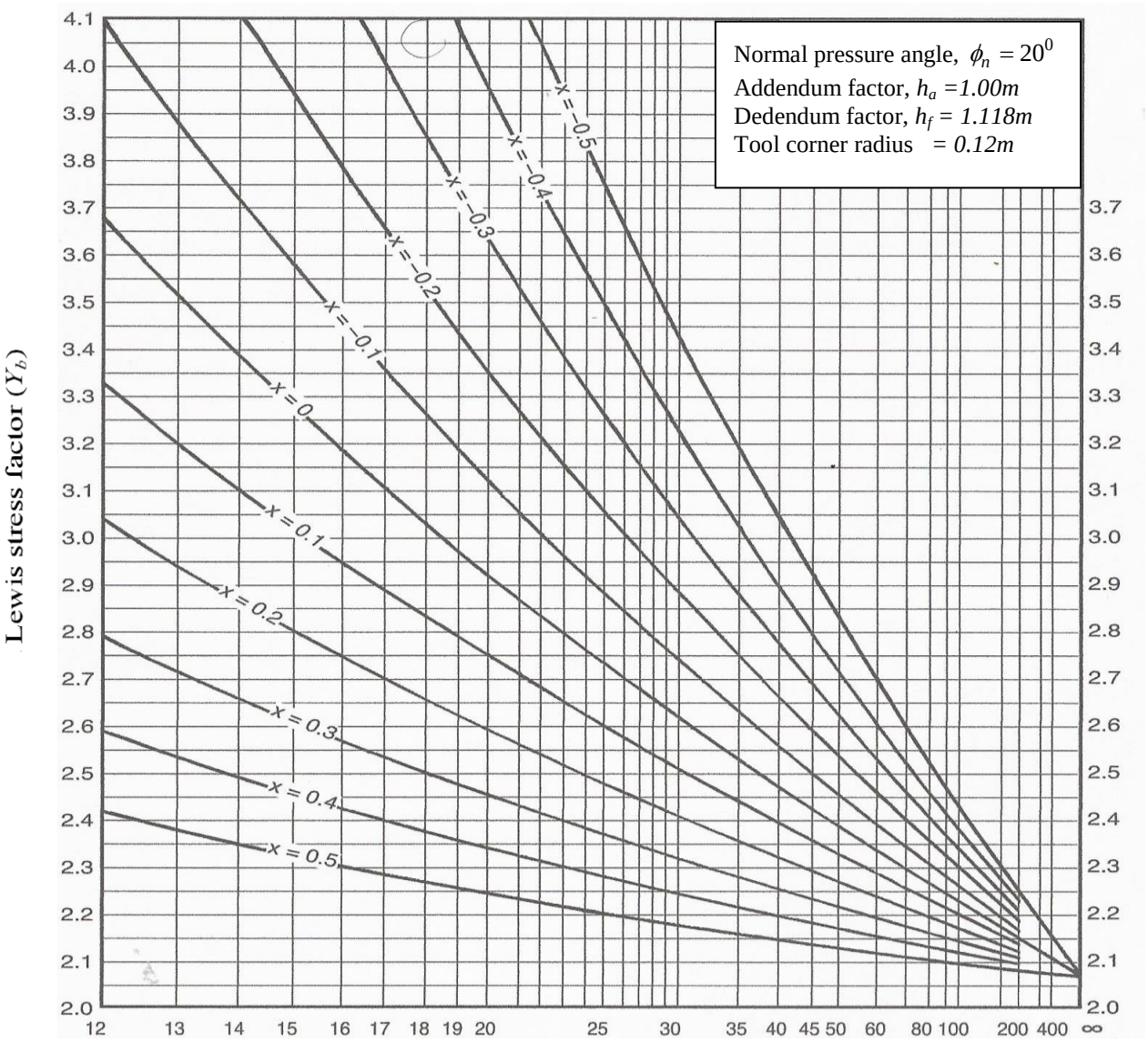

Fig. 2: Lewis stress factor for straight bevel gears [15, 37]